

On the derivation of the Tully-Fisher relations

II. Field galaxies, the inverse TF slope and the Hubble constant

T. Ekholm and P. Teerikorpi

Tuorla Observatory, University of Turku, FIN-21500 Piikkiö, Finland

Received 24 October 1996 / Accepted 11 March 1997

Abstract. The Hubble constant H_0 should not show distance-dependence. An inappropriate use of the direct Tully-Fisher relation may lead to a conclusion that H_0 is dependent on the distance. This paper tries to answer the question: is it possible to avoid the caveats of the direct relation by applying the inverse Tully-Fisher relation. Under ideal conditions it is possible simultaneously to determine the inverse slope precisely and to find the Hubble constant next to calibration. Ideal conditions are, however, rarely met. Two particular sources of error in the resulting average Hubble constant are considered. A progressive measurement error in angular diameters (apparent magnitudes) causes overestimation of H_0 . An asymmetry in the $\log V_{\max}$ -distribution in the sense of a tail of small rotational velocities tends to shift H_0 upwards.

Key words: distance scale

1. Introduction

The knowledge on the use of the Tully-Fisher (TF) dependence between the absolute magnitude M (or the linear diameter) and the maximum rotational velocity V_{\max} in problems involving distance determinations has improved and matured during the several last years. This is true for both the so-called direct and inverse relations. However, the theoretical studies have usually been conducted under rather idealized conditions involving e.g. the possession of a true magnitude limited sample and the knowledge of the relevant direct and inverse slopes. One also usually presumes that there is no selection pressure towards high or small V_{\max} at a given constant M , that the dispersions follow a gaussian law, that there is one TF relation for all galaxy types and so on. In practice all such assumptions are problematic.

For example, a large, statistically significant sample is by its nature a merger of sources of incoherent selection criteria and measurements of different accuracy (magnitude, diameter, observed redshift, Hubble type etc.). As a result, the gain in numbers may be obliterated by heterogeneity and hidden biases. As another example, $\log V_{\max}$ (hereafter $p = \log V_{\max}$) may not

have a strictly gaussian or even symmetric distribution around a fixed M . Only an approximate slope is known and in any application a slope differing from the true (or relevant) slope by some error is implemented. Some first steps in discussing problems of this kind were made in Paper I (Ekholm 1996) where Monte Carlo simulations were conducted in order to study the influence of a synthetic inhomogeneity on the derivation of the TF relations using field galaxies. Here we proceed to study the influence of these problems. Like Paper I, the present work is a natural continuation of a series of papers where the TF distance moduli, both direct and inverse, and the biases involved have been addressed (cf. Teerikorpi 1993 for references). In thinking of the various problems approached either analytically or numerically, we have in mind applications to such large data sets as in the KLUN project (Kinematics of the Local Universe; Paturel et al. 1994). At the same time, we try to appreciate that the theory of distance indicators is a fascinating subject as such, deserving a systematic treatment.

We study how to use the inverse TF approach for the determination of the Hubble constant, with the understanding that this is only one important application coming out of the present discussion. We address the questions of the slope, the gaussian dispersion and sample incompleteness, and ask whether there is an inverse TF counterpart for the Spaenhauer diagram, recently much utilized by Sandage and his collaborators (cf. Sandage 1994a, 1994b) for eliminating the bias in the direct TF (or equivalent) relation, or whether the method of normalized distances, together with the “unbiased plateau” in the H_0 vs. d_{norm} diagram (Bottinelli et al. 1986) offers any insight to the use of the inverse TF relation. Both of these methods are concerned with the Malmquist bias of the second kind (a terminology proposed by Teerikorpi 1995), seen as changes in the average absolute magnitude $\langle M \rangle$ or in the Hubble parameter H with increasing true distance, when a magnitude limited sample is used.

Because different inverse slopes will be referred to, it is necessary to define each with a unique notation. A theoretical slope a' means the slope in

$$p = a'M + b', \quad (1)$$

where the absolute magnitude M is a true value without any error and p has been correctly deduced from the data for every M . In practice such a slope might be approached by a slope a'_c deduced from a properly constructed, sufficiently large calibrator sample or from a distant cluster with accurately measured (apparent) magnitudes. Here we are especially interested in the slope a^* derived from field galaxies using kinematic distances inferred from some more or less accurate model. Errors in relative distances cause errors in M , which tend to make a^* shallower than a' or a'_c .

This paper is structured as follows. In Sect. 2 the hypothesis “the inverse relation causes the unbiased plateau in the average Hubble ratio vs. kinematic distance diagram to extend over all distances” is tested. In Sect. 3 it is shown how one may simultaneously fine-tune the inverse slope and obtain an unbiased estimate for the Hubble ratio. In Sect. 4 the bias arising from the larger contribution of small galaxies being less accurately measured is discussed. In Sect. 5 an “inverse Spaenhauer diagram” is introduced. It is also shown how such a diagram may be used for deriving the inverse TF parameters even in the presence of non-gaussian errors. In Sect. 6 some aspects of an asymmetric p -distribution are discussed. Finally, in Sect. 7 the conclusions are summarized.

2. The Hubble ratios from the inverse slope

One route to the Hubble constant H_0 , next to calibration, using field galaxies and the direct TF relation, was described by Bottinelli et al. (1986). In the method of normalized distances individual Hubble ratios $H_0 = V_{\text{linear}}/d_{\text{photo}}$ are plotted against the normalized kinematic distance d_n defined so that for each p equally large bias occurs at each d_n . The normalization allows one to determine an unbiased plateau, i.e. the range of d_n in which the (2nd) Malmquist bias vanishes. V_{linear} refers to a velocity expected from a linear velocity-distance law $V = H_0 \times r_{\text{Virgo}} \times d_{\text{kin}}$, where d_{kin} is calculated implementing some kinematic model assumed to reasonably well approximate the underlying velocity field. The photometric (or diameter) distance d_{TF} is inferred from the direct Tully-Fisher relation $M = ap + b$. The slope of the direct relation has often been calculated from the data in the unbiased plateau itself, which requires an iteration process (e.g. Theureau et al. 1997b). On the other hand, in Paper I it was shown that extending the data somewhat beyond the unbiased plateau does not influence much the derived slope (though naturally there is a continuous shift in the zero-point b because of the Malmquist effect).

The necessity of restricting the sample to the unbiased plateau is a problem with the direct TF relation, how natural as a distance indicator it may be. This restriction leads to a “loss” of a large majority of the data in the determination of H_0 . One is led to ask about the prospects of using the inverse TF relation $p = a'M + b'$, where – in principle – all data may be used (in fact, should be used with no restriction on p). Theoretically, it is known that the inverse TF distances are free from the Malmquist bias of the 2nd kind, i.e. $\langle d_{\text{TF}} \rangle$ is unbiased on each constant true distance. No normalization is needed, and the unbiased plateau

may be thought to extend to all distances in a H vs. d_{kin} diagram. However, it must be emphasized that the mentioned – quite famous – property of the inverse Tully-Fisher relation crucially depends on the *presumption* that for each absolute magnitude M the distribution of rotational velocities, $\phi_M(p)$, is complete. In most treatises on the inverse relation this presumption has been more or less explicitly assumed to be valid. Also, it is usually assumed that the distribution $\phi_M(p)$ is gaussian:

$$\phi_M(p) = \frac{1}{\sqrt{2\pi}\sigma_p} \exp\left[-\frac{(p - p(M))^2}{2\sigma_p^2}\right]. \quad (2)$$

For the time being we assume that $\phi_M(p)$ obeys Eq. (2), and that for the average value $\langle \phi_M(p) \rangle = p(M)$ some intrinsically valid relation $p = a'M + b'$ exists.

It is also worth mentioning, that the larger sample available for the inverse TF study is counteracted by the fact that the dispersion of individual H values is larger than that coming from the direct TF distance moduli (in the unbiased plateau). The relevant dispersion is σ_p/a' , related to σ_{M_p} via

$$1/(\sigma_p/a')^2 = 1/\sigma_{M_p}^2 - 1/\sigma_M^2, \quad (3)$$

where σ_M is the dispersion in the general luminosity function.

The inverse TF distance moduli are derived from $M = (p - b')/a' = A'p + B'$. Both A' and B' are bound to have some error due to determination of the slope a' and the zero-point b' calibration. It is natural to ask what is the influence of the erroneous parameter values on the derived average Hubble ratio.

In logarithmic form one writes the Hubble parameter that would have been derived from an accurate TF relation $M_{\text{inv}} = A'p + B'$ as

$$\log H_0 = \log V_{\text{linear}} - 0.2m + 0.2(A'p + B') + 5, \quad (4)$$

while in practice one has values $A = 1/a^*$ and $B = -b^*/a^*$:

$$\log H_0^* = \log V_{\text{linear}} - 0.2m + 0.2(Ap + B) + 5. \quad (5)$$

Subtraction of these equations yields the difference in the individual Hubble ratios $\Delta H = \log H_0^* - \log H_0$:

$$\Delta H = 0.2\left[A'\left(\frac{A}{A'} - 1\right)p + (B - B')\right]. \quad (6)$$

The average of ΔH at each kinematic distance (in fact, the error in the average derived $\log H$) clearly depends on the average p at that distance, $\langle p \rangle_{d_{\text{kin}}}$. The average value can be calculated using the following argument. Galaxies at d_{kin} have an average $\langle M \rangle_{d_{\text{kin}}}$, which is basically determined by the magnitude limit and the luminosity function. $\langle p \rangle_{d_{\text{kin}}}$ is obtained from this value via the accurate inverse TF parameters A' and B' as:

$$\langle \Delta H \rangle_{d_{\text{kin}}} = 0.2\left[\left(\frac{A}{A'} - 1\right)\langle M \rangle_{d_{\text{kin}}} - \frac{AB'}{A'} + B\right]. \quad (7)$$

On the qualitative level the predictions of the Eq. (7) are obvious: an erroneous derived zero-point $B \neq B'$ predicts an erroneous Hubble ratio for $A = A'$ by an amount $-0.2(B - B')$,

as expected, while an adopted slope $A \neq A'$ predicts an unreal tendency for the Hubble constant of being a function of distance. A special example would be to use simply the direct TF slope, being always $A/A' < 1$ and resulting – as is well known – in a progressively increasing Hubble parameter. *Only under the extremely constraining condition $A/A' = 1$, is the statement on the distance-independent unbiased plateau valid.* It is also worth mentioning that the error in the inverse slope induces the influence of the magnitude limit via $\langle M \rangle_{d_{\text{kin}}}$ into the average Hubble ratio. It is again a healthy reminder that the maxim “unbiased distances can be inferred from the inverse relation” should be apprehended with caution. The result is not surprising if understood as reflecting the fact that the inverse relation was used in a “direct sense”. Neither is it surprising if recalling that Teerikorpi (1984) proved that the inverse Tully-Fisher distances are unbiased on average presuming the relation $p(M) = a'M + b'$ is correctly derived from the local data.

Eq. (7) takes a simpler form if one adds a successful calibration. Now the zero-point B can be expressed in terms of A , A' and B' . It is required that the average calibrator $\langle M \rangle_c$ predicts same $\langle p \rangle$ for the adopted relation (A, B) and for the accurate relation (A', B') , i.e.

$$\frac{\langle M \rangle_c - B}{A} = \frac{\langle M \rangle_c - B'}{A'},$$

from which one writes

$$B = \left(1 - \frac{A}{A'}\right) \langle M \rangle_c + \frac{A}{A'} B'. \quad (8)$$

Substitution of Eq. (8) into (7) yields the final result

$$\langle \Delta H \rangle = 0.2 \left(\frac{A}{A'} - 1 \right) (\langle M \rangle_{d_{\text{kin}}} - \langle M \rangle) \quad (9)$$

Note the resemblance of Eq. (9) with Eq. (15) in Teerikorpi (1990), where biased cluster distances from the inverse TF relation were discussed. However, in that treatise the relevant slope was erroneous because of different accuracies of the calibrator and sample magnitudes, while here a truly erroneous slope was forced on the calibrator data. Note also that when using the direct relation the calibrators must represent a truly volume-limited sample. *When implementing the inverse relation in the ideal case ($A = A'$) it does not matter whether the calibrators are selected from a volume-limited or a magnitude-limited sample as can be seen e.g. from Eq. (9).* We emphasize this point, because usually the same set of calibrators is used for both the direct and the inverse TF-relation.

3. Fine-tuning the slope and determining H_0

How does Eq. (9) read if the influence of the magnitude limit on $\langle M \rangle_{d_{\text{kin}}}$ is taken into account? Using $M_1 = m_1 - 5 \log d_{\text{kin}} - 25$ one can solve the average absolute magnitude as a function of distance from

$$\langle M \rangle_{d_{\text{kin}}} = \frac{\int_{-\infty}^{M_1} dM M \Phi(M)}{\int_{-\infty}^{M_1} dM \Phi(M)}, \quad (10)$$

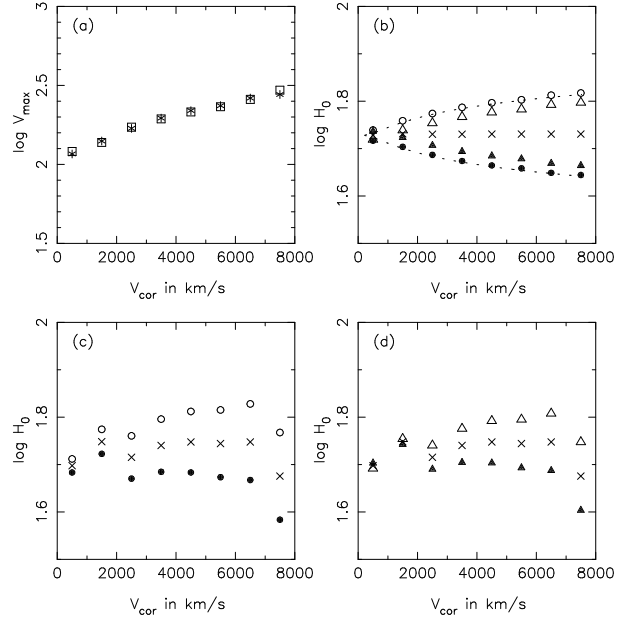


Fig. 1a–d. Examples demonstrating the influence of an erroneous inverse slope on resulting $\log H_0$.

adopting a gaussian luminosity function $\Phi(M)$ and noting that $\langle \Delta H \rangle = \langle \log H_0^* \rangle_{d_{\text{kin}}} - \langle \log H_0 \rangle_{d_{\text{kin}}}$. The error in the derived Hubble ratio can be expressed in terms of the magnitude limit

$$\langle \Delta H \rangle_{d_{\text{kin}}} = \left(\frac{A}{A'} - 1 \right) \frac{0.4\sigma \exp[-(M_1 - \langle M \rangle)^2 / 2\sigma^2]}{\sqrt{2\pi} (1 + \operatorname{erf}[(M_1 - \langle M \rangle) / \sqrt{2}\sigma])} \quad (11)$$

Fig. 1 illustrates the results obtained in Sect. 2. As in Paper I we utilize a synthetic Virgo supercluster. We assume a gaussian luminosity function with $M_0 = -18.6$ and $\sigma_M = 1.4$. The sample was imposed to a magnitude limit $m_{\text{lim}} = 13.25$. The number of galaxies left was $N = 746$. First consider the “ideal” case where $p = a'M + b'$ with $a' = -0.1$ and $b' = 0.15$. This case refers to the argument used in the derivation of Eq. (7) (for each d_{kin} $\langle p \rangle = a'\langle M \rangle + b'$). The average $\langle p \rangle_{d_{\text{kin}}}$ are shown in Fig. 1a as stars. In Fig. 1b we demonstrate the behavior of $\langle H_0 \rangle$ as a function of distance for $A/A' = 1.1$ (bullets), $A/A' = 1.0$ (crosses) and $A/A' = 0.9$ (circles). The sample used was calibrated by Eq. (8) assuming that the “calibrator sample” is volume-limited, i.e. $\langle M \rangle_c = M_0$. The dotted lines give the theoretical predictions of Eq. (11) for $A/A' = 1.1$ and $A/A' = 0.9$. The solid and open triangles demonstrate what happens if the calibrator sample is magnitude-limited ($\langle M \rangle_c = -19.6$). If the slope is too shallow $\log H_0$ is underestimated and if the slope is too steep $\log H_0$ is overestimated. For the correct slope it does not matter whether the calibrator sample is volume or magnitude-limited.

Eq. (11) and Fig. 1b have special significance for the determination of H_0 using the inverse Tully-Fisher relation. One might be content to derive the slope A e.g. from field galaxies or from a cluster, force it on the calibrators and get $\langle \log H_0 \rangle$ from a large field galaxy sample. However, as any such determination is accompanied by an error in the slope, there will be a systematic deviation according to Eq. (11). This error may go

unnoticed if one does not analyze the behavior of $\langle \log H_0 \rangle$ as a function of the kinematic distance. The first choice for A , possibly showing a trend away from the horizontal line in the $\log H_0$ vs. d_{kin} diagram, may then be adjusted to let this trend disappear. Simultaneously, and rather remarkably, such a fine-tuning of the slope brings about an unbiased estimate for $\log H_0$.

In Fig. 1c and 1d we show the results for an ‘‘actual’’ sample, where $p = 0.1N(0, 1) + a'M + b'$ and $N(0, 1)$ is a normalized gaussian random variable. The resulting average values are plotted to Fig. 1a as open squares. Even as the theoretical prediction should still yield for each d_{kin} $\langle p \rangle = a'\langle M \rangle + b'$, the averages show deviations from this prediction. This is because of the incomplete sampling of $\log V_{\text{max}}$'s. The sampling is effectively a Poisson process by its nature. If one would carry out a Monte Carlo simulation using, say, 100 realizations, it is expected that deviations would cancel out. In practise we have one realization leading to the distortions seen in Figs. 1c and 1d as compared to Fig. 1b. Difficulties aroused by this fact can be avoided or at least diminished by the implementation of a normalized inverse Spaenhauer diagram described in Sect. 5.

4. Measurement errors

So far it has been assumed that the magnitudes (or diameters) have been accurately observed. There is a source of error which is especially important for the inverse slope method, where all galaxies are included, with high weight for the apparently small ones having large measurement errors. The essence of this problem is the increasing number of galaxies with small diameters. When one constructs a diameter limited sample out of galaxies already measured, the measurement errors tend to shift galaxies upwards on the apparent diameter axis – on the average the diameters become too large. It is worth mentioning that if one now repeats the measurements for the limited sample, the bias vanishes. Galaxies for each apparent angular diameter have equal probability of being measured as too large or as too small. In terms of Gould's (1993) effect, the influence of the first and second measurement errors vanishes from Gould's covariance because of their independence. Of course, for large samples like the KLUN sample it is impractical to request for repeated measurements. Thus one should understand the origin and properties of this type of bias on a more formal basis.

Consider a uniform spatial distribution of galaxies. The distance moduli are then distributed as $f(\mu) \propto 10^{0.6\mu}$. Note however that the uniformity is not a crucial assumption. One might as well consider any distribution of the form $f(\mu) \propto 10^{0.2(3-\alpha)\mu}$. Because the formal treatment is similar for both the magnitudes and diameters, the apparent quantity is labeled as x and absolute counterpart as X . Assume now that the correct x (x'), is observed with an accuracy σ_x and that the observed values are normally distributed around x' . It is now asked with what probability would a galaxy being observed to have x actually have x' .

This bayesian probability is expressed as

$$P(x' | x) = \frac{P(x')P(x | x')}{\int_{-\infty}^{+\infty} dx' P(x')P(x | x')} \quad (12)$$

The probability density function $P(x')$ for the magnitudes is $P(x') = \exp(\beta m')$ ($\mu = m - M$), where $\beta = 3 \ln 10/5$, and for the diameters $P(x') = \exp(-5\beta \log D'_{25})$ ($0.2\mu = \log D - \log D_{25}$). We write: $P(x') = \exp(\alpha x')$ with $\alpha = \beta$ for the magnitudes and $\alpha = -5\beta$ for the diameters. As defined above

$$P(x | x') = \frac{1}{\sqrt{2\pi}\sigma_x} \exp\left[-\frac{(x - x')^2}{2\sigma_x^2}\right]. \quad (13)$$

Thus, $P(x')P(x | x')$ is expressed as

$$\exp[\alpha(x + \alpha\sigma_x^2/2)] \exp\left[-\frac{(x - x' + \alpha\sigma_x^2)^2}{2\sigma_x^2}\right],$$

and the quantity required, the expectation value

$$E(x' | x) = \int_{-\infty}^{+\infty} dx' x' P(x' | x),$$

can be written in the form

$$E(x' | x) = \frac{\int_{-\infty}^{+\infty} dx' x' \exp[-(x - x' + \alpha\sigma_x^2)^2/2\sigma_x^2]}{\int_{-\infty}^{+\infty} dx' \exp[-(x - x' + \alpha\sigma_x^2)^2/2\sigma_x^2]}. \quad (14)$$

We first note that as $\sigma_x \rightarrow 0$, Eq. (14) goes

$$E(x' | x) \rightarrow \frac{\int_{-\infty}^{+\infty} dx' x' \delta(x - x')}{\int_{-\infty}^{+\infty} dx' \delta(x - x')} = x,$$

as indeed it should.

The usual change of variables $t = (x - x' + \alpha\sigma_x^2)/\sqrt{2}\sigma_x$ yields:

$$E(x' | x) = x + \alpha\sigma_x^2 - \sqrt{2}\sigma_x \frac{\int_{-\infty}^{+\infty} dt t \exp[-t^2]}{\int_{-\infty}^{+\infty} dt \exp[-t^2]}. \quad (15)$$

As the last term containing the integrals vanishes, one writes the correction term for the magnitudes as

$$\epsilon_m = (3 \ln 10/5) \sigma_m^2, \quad (16)$$

and for the diameters as

$$\epsilon_D = -3 \ln 10 \sigma_D^2. \quad (17)$$

By comparing the expectation values one notes that it is more probable to have included in the sample a galaxy which has been measured as too large (too bright). These formulae are formally identical with the classical Malmquist bias, though here σ refers to the error in measurement, while classically it is the dispersion in intrinsic properties. For example, Eq. (17) means that for a given true linear diameter $\log D$ galaxies are measured to have on average too large angular diameters $\log D_{25}$ predicting a too short distance scale and a too large Hubble constant.

Consider Eq. (5) for the measured $\log H_0^*$. By taking the averages it reads for a constant $\log V_{\text{linear}}$ as:

$$\langle \log H_0^* \rangle = \log V_{\text{linear}} - 0.2 \langle m \rangle + 0.2(A \langle p \rangle + B) + 5. \quad (5')$$

Here $\langle m \rangle = \langle m' \rangle - \langle \epsilon_m \rangle$ with m' being the correct apparent magnitude and ϵ_m is given by Eq. (16). The predicted $\langle M \rangle = A \langle p \rangle + B$ depends on the values assigned to the inverse parameters A and B .

Suppose that the derived slope A reflects the accurate slope A' , i.e. $A = A'$ and that the inverse relation has been properly calibrated: $B = B'$. Now $\langle p \rangle$ predicts the true $\langle M' \rangle$ and Eq. (5') yields:

$$\langle \log H_0^* \rangle = \langle \log H_0 \rangle + \langle \epsilon_m \rangle. \quad (18)$$

In the derivation of Eq. (18) it was presumed that V_{linear} genuinely reflects the true distance modulus $\langle \mu' \rangle = \langle m' \rangle - \langle M' \rangle$.

Similar results are, of course, valid for the inverse diameter TF-relation. It is perhaps worth mentioning that the importance of this kind of a statistical error has been recently discussed by Perryman et al. (1995) in connection with the stellar parallaxes (their Sect. 4). As a matter of fact the influence of the measurement errors on the stellar parallaxes can be traced back to a paper by Dyson (1926), where he refers to a solution given by Eddington.

5. The inverse Spaenhauer diagram

The correctness of the inverse TF-slope derived using least squares basically depends on i) $\phi_X(p)$ is gaussian in form and complete for each X (X denoting M or $\log D$ and ii) the apparent x and the distance modulus μ from which X is calculated are without errors. Some remarks on the second requirement were made in Sect. 4.

As regards the first requirement we ask whether one could here apply the concept of a Spaenhauer diagram promoted by Sandage (1994a, 1994b). In the “direct” Spaenhauer diagram one studies the X -distribution as a function of distance for each p . In a similar fashion one may construct an “inverse” Spaenhauer diagram, i.e. study the properties of $\phi_X(p)$ for each X . As demonstrated by Theureau et al. (1997a) the observed p 's reflect different X for different Hubble types T . In fact, the inverse relation should be expressed as $p = a'X + b'(T)$. In practical terms, the division of the sample according to their types may lead into so small numbers of galaxies in some X -bins that one cannot judge whether any intrinsic selection in p exists.

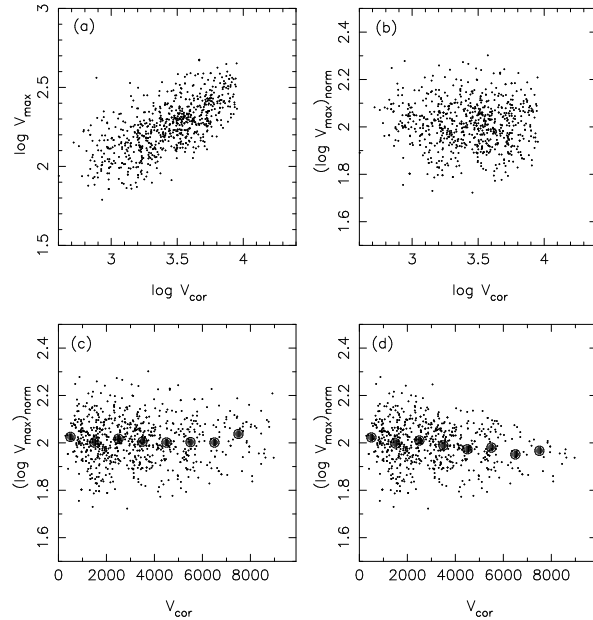


Fig. 2a–d. Schematic diagrams showing the practical use of a normalized inverse Spaenhauer diagram.

If, however, it is plausible to assume that “for all X the distribution $\phi_X(p)$ is symmetric around X and of the same form” one may overcome this problem by normalizing the observed p 's to a common X_n via

$$p_n = p - a'_n(X - X_n). \quad (19)$$

Assume that each X is calculated from the correct values x' and d' . This true value of X is labelled as X' . Because $p = a'X' + b'(T)$ we can express the resulting average of p_n at each true distance d' in terms of the average X' at that distance as

$$\langle p_n \rangle_{d'} = (a' - a'_n) \langle X' \rangle_{d'} + a'_n X_n + b'(T). \quad (20)$$

Now, for a steeper normalization slope ($a'_n > a'$), the normalized average $\langle p_n \rangle_{d'}$ is expected to decrease as a function of distance and, for a shallower slope, to increase. Hence, the diagram could be used for demonstrating the error in the slope. It is worth mentioning that this “normalized inverse Spaenhauer diagram” can also be used as a diagnostics for a possible zero-point difference between different population because of the explicit $b'(T)$ dependence (for an example cf. Fig. 5 in Theureau et al. 1997a).

So far the appearance of the diagram was studied presuming a priori knowledge of the correct slope. As clearly demonstrated in Sect. 3 an erroneous slope immediately induces biased distances into the average derived distance vs. true distance diagram. One may now ask whether the bias vanishes if the normalization slope resulting in constant $\langle p_n \rangle_{d'}$ is applied. By defining the error in the derived distance d_{der} relative to the true distance as $\Delta d = 5 \times (\langle \log d_{\text{der}} \rangle - \langle \log d' \rangle)$ one may write by denoting $\langle X' \rangle = A' \langle p \rangle + B'$ and $\langle X \rangle = A \langle p \rangle + B$,

$$\Delta d = (A' - A) \langle p \rangle + (B' - B). \quad (21)$$

The average p is expressed in terms of the average X' at a given d' as $\langle p \rangle = (\langle X' \rangle - B')/A'$, which when substituted into Eq. (21) yields

$$\Delta d = \left(1 - \frac{A}{A'}\right)\langle X' \rangle + \frac{A}{A'}B' - B. \quad (22)$$

Consider now the normalized average p :

$$\frac{\langle X' \rangle - B_n}{A_n} = \frac{\langle X' \rangle - B}{A} - \frac{\langle X' \rangle - X_n}{A_n},$$

from which one writes

$$A\langle X' \rangle = AB_n + A_n\langle X' \rangle - A_nB - A(\langle X' \rangle - X_n). \quad (23)$$

Now, if the normalization was indeed properly carried out i.e. $a'_n = a'$, Eq. (20) yields $\langle X' \rangle - X_n = B_n - B'$. When substituted into Eq. (23) one gets

$$A\langle X' \rangle = A'\langle X' \rangle - A'B + AB'. \quad (24)$$

One immediately sees that substitution of Eq. (24) into Eq. (22) makes the error equal to zero. This simple proof confirms what could have been intuitively deduced from the arguments given earlier in this section. Furthermore, in this method of *fine-tuning* the inverse slope no assumption of the normalcy of the distribution $\phi_M(p)$ is needed. All required is that the distribution is symmetric.

How does one use the inverse Spaenhauer diagram in practice? In Fig. 2. schematic examples are shown using the ‘‘actual’’ sample of Sect. 3. The resulting inverse Spaenhauer diagram is shown in panel (a). In panel (b) is the resulting normalized diagram. The normalizing parameters were $a'_n = -0.1$ and $M'_n = -18.6$. At the bottom row in the panel (c) the average p_n 's (balls) are calculated for galaxies having $V \geq 1000 \text{ km s}^{-1}$ and $V < 8000 \text{ km s}^{-1}$ with bin size 1000 km s^{-1} . From this panel one can see how the $\langle p_n \rangle$'s follow quite well a horizontal line (as they indeed should, because the normalization slope equals the input ‘‘true’’ slope). In the panel (d) the effect of a selection cut-off at $p = 2.45$ can be seen. As the lower edge of the distribution stays horizontal more and more points at the upper edge are missed as the distance increases. Note also how the average p_n 's declines as a function of distance.

6. Implications of an asymmetric $\log V_{\text{max}}$ -distribution

In the previous section it was proved that by implementing the ‘‘inverse Spaenhauer diagram’’ it is possible to determine the inverse slope even when the p -distribution is not gaussian in form. It was, however, required that the distribution is symmetric. In order to complete the discussion we address the question of the implications of an asymmetric distribution.

Theureau et al. (1997a) tried to understand the inverse TF-relation in terms of a simple mass model. In the model the mass responsible for V_{max} , M_{tot} , is decomposed into the mass of the luminous matter in the disk, M_d , the mass of the bulge, M_b and the mass of the dark halo, M_h . Following Theureau et al. (1997a)

we assume that at the radius r_{max} where V_{max} is measured, the sum $M_b + M_h$ can be expressed as a fraction of the total mass βM_{tot} . We write

$$V_{\text{max}}^2 \propto M_d/(1 - \beta) = cM_d. \quad (25)$$

Suppose now, as a first approximation, that the disk mass M_d has at r_{max} a gaussian distribution around μ with dispersion σ . Thus the square of the maximum rotational velocity V_{max} has a gaussian distribution around $c\mu$ with dispersion $c\sigma$.

For computational convenience we assume, for the time being, that V_{max}^2 depends purely on the disk mass M_d , i.e. $c = 1$ and, that $p = \ln V_{\text{max}}$ instead of $\log V_{\text{max}}$. We now ask what is the distribution of the logarithmic quantity p .

In general, if a random variable Y is obtained from a random variable X obeying a distribution $f_X(x)$ via a transformation $Y = g(X)$, the cumulative distribution function is

$$F_Y(y) = F_X(g^{-1}(y)).$$

By denoting $X = V_{\text{max}}^2$, one writes

$$Y = \ln \sqrt{X} = \ln X/2 \Leftrightarrow X = e^{2y},$$

thus leading to

$$F_Y(y) = F_X(e^{2y}). \quad (26)$$

Differentiation of both sides of Eq. (26) yields:

$$f_Y(y) = \phi(p) = 2e^{2p} f_X(e^{2p}). \quad (27)$$

The assumption that the distribution function of X , $f_X(x)$, is normal allows one to express Eq. (27) as

$$\phi(p) = \sqrt{\frac{2}{\pi}} \frac{e^{2p}}{\sigma} \exp\left[-\frac{(e^{2p} - \mu)^2}{2\sigma^2}\right]. \quad (28)$$

What are the implications of Eq. (28) as regards the determination of the Hubble constant H_0 ? The maximum of the distribution $\phi(p)$ is found at

$$p_{\text{max}} = \frac{1}{2} \ln \left(\frac{\mu}{2} + \sqrt{\frac{\mu^2}{4} + \sigma^2} \right). \quad (29)$$

Now consider the probability of finding galaxies with $p < \ln \mu/2$:

$$P(p < \ln \mu/2) = \int_{-\infty}^{\ln \mu/2} dp \sqrt{\frac{2}{\pi}} \frac{e^{2p}}{\sigma} \exp\left[-\frac{(e^{2p} - \mu)^2}{2\sigma^2}\right],$$

which after the change of variable $t = e^{2p}$ yields:

$$P(t < \mu) = \int_0^{\mu} dt \sqrt{\frac{2}{\pi}} \frac{1}{\sigma} \exp\left[-\frac{(t - \mu)^2}{2\sigma^2}\right] = \mu \quad (30)$$

One directly sees that $P(p < \ln \mu/2) = \ln \mu/2$. Eq.(30) gives the median of the distribution and thus we conclude together

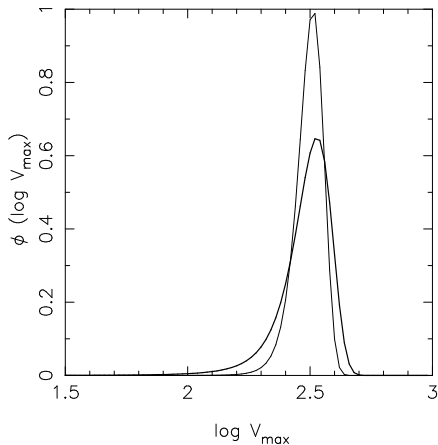


Fig. 3. Examples of Eq. (27). Both distributions have $c\mu = 10^5 \text{ km s}^{-1}$. They have dispersions $c\sigma = 2.5 \times 10^4 \text{ km s}^{-1}$ and $c\sigma = 4.0 \times 10^4 \text{ km s}^{-1}$ (the bold curve). The distributions are normalized to the maximum value p_{\max} for $c = 2.5$.

with Eq. (29) that the inverse zero-point b' if derived using least squares is underestimated. This is a result of the fact that in this case b' reflects the average of the distribution $\phi(p)$. The asymmetry in $\phi(p)$ repeats itself in the asymmetry of the distribution of the zero-points $\phi(b')$ and in the distribution of the $\log H_0$'s being proportional to the distribution $\phi(B') = -\phi(b')/a'$. The average Hubble constant

$$\langle H_0 \rangle = 10^{\langle \log H_0 \rangle} \quad (31)$$

is predicted to be too large.

If one now uses $p = \log V_{\max}$ and allows for the influence of the bulge+halo component ($c \neq 1$), one rewrites Eq. (28) as

$$\phi(p) = 2 \ln 10 \frac{10^{2p}}{\sqrt{2\pi}c\sigma} \exp\left[-\frac{(10^{2p} - c\mu)^2}{2c^2\sigma^2}\right]. \quad (28')$$

In Fig. 3 two examples of the distribution given by Eq. (28') are shown. For both cases the ‘‘intrinsic’’ dispersion of the rotational velocity squared is assumed to be $\sigma = 10^4 \text{ km s}^{-1}$, modified by $c = 2.5$ and $c = 4.0$ (bold line). For simplicity, the average was assumed to be same both cases $c\mu = 10^5 \text{ km s}^{-1}$. The distributions are normalized to the maximum value p_{\max} for $c = 2.5$. It is interesting to note how the tail of small values of p becomes more prominent as the initial distribution becomes broader.

Finally, it is worth emphasizing that the model used here should be considered as a means to create an asymmetry in the distribution of p 's rather than as an attempt to describe the underlying physics. We try to understand the ramifications of an asymmetric distribution: a tail of small p -values results in a too large Hubble constant.

If the p -distribution indeed has such an intrinsic asymmetry, also the calibrators suffer from it. Different types may have different distributions because of the influence of the dispersion. The inverse counterparts of the equations given in the Appendix of Theureau et al. (1997b) may thus lead to an incorrect calibration. The primed quantities in their Eqs. (A.1a) and (A.1b)

depend on the shift in the zero-points $\Delta b' = b'(6) - b'(T)$. If the zero-points are derived using least-squares method they must contain some error. As the tail of small p 's become more and more prominent, the zero-point b' becomes more and more underestimated.

Note also that even in the case of a single type when the calibration should succeed, the asymmetric distribution of the individual zero-points B' result in an overestimation of the Hubble constant H_0 . In the symmetric case the average $\langle \log H_0 \rangle$ reflects the median of the H_0 -distribution (cf. Eq. (31)). It is as probable to observe a larger value than this as it is to observe a smaller one. The tail of large individual Hubble parameters yield an average $\langle \log H_0 \rangle$ larger than the corresponding median. Eq. (31) is no longer valid.

We have discussed this point and the measurement errors in Sect. 4., because tentative experiments with the inverse TF relation and the KLUN sample have revealed an asymmetric distribution of $\log H_0$ and a larger derived H_0 than obtained by Theureau et al. (1997b) using the direct TF relation.

7. Summary

In this paper aspects of the derivation of the Hubble ratio using the inverse Tully-Fisher relation were considered. Particular attention was paid to the validity of a hypothesis that the unbiased plateau in the average Hubble ratio vs. kinematic distance diagram covers all distances and hence no normalization of the distances is needed. This hypothesis is based on the theoretical result that the inverse Tully-Fisher relation predicts unbiased average distances for each true distance. Teerikorpi (1984) states that if a linear relation between the absolute magnitude or the linear diameter exists, then *when this relation is correctly reproduced from the data* the Malmquist bias of the second kind vanishes on average.

As a starting point it was assumed that a kinematic model predicts such true distances. In the introduction it was pointed out that the least squares solution does not *necessarily* return the correct relation. In Sect. 2 it was shown that only when the error in the inverse slope vanishes is the hypothesis valid. If the derived slope is shallower than the correct one increase in the Hubble ratio is expected, and if it is steeper decrease is expected. It was also shown how the error in the slope induces the influence of the magnitude limit into the average Hubble ratio. This result is not surprising, because the inverse relation was used in a ‘‘direct’’ sense. It was also emphasized that the maxim ‘‘unbiased distances can be inferred from the inverse relation’’ should be apprehended with caution. The derived distances are unbiased only when the derived inverse slope equals the correct one.

Why do we emphasize this point? Should one not be equally careful with the direct slope? Indeed, but because the Malmquist biases are always present when implementing the direct Tully-Fisher relation, one usually pays considerable attention to proper derivation of it. In an inverse TF-distance vs. velocity diagram one may accept the theoretical conclusion of the bias of the 2nd kind to vanish on average by its face-value without appreciating that at extreme values of p (fastest rotators probing large

distances) even a small error in the inverse slope may be devastating.

When the derived zero-point is forced to the solution obtained from the calibrators the error in the derived Hubble ratio vanishes in the complete, distance-limited sample. This is not surprising, because a successful calibration should yield the correct relation for such sample.

Depending on the magnitude limit, the erroneous slope may have a rather important influence on the inferred inverse distances and thus on the derived Hubble ratio. The brighter the limit, the larger the error. Some examples of the behavior were shown in Fig. 1 in Sect. 3. If one finds a trend away from the horizontal line in the $\log H_0$ vs. d_{kin} diagram, one may adjust the inverse slope to let this trend disappear. This adjustment simultaneously brings about an unbiased estimate for $\log H_0$. This is a new and quite remarkable property of the Hubble diagram.

The results summarized so far are valid under ideal conditions. In Sect. 4 we asked how a progressive measurement error increasing towards small galaxies influences the derived value of H_0 . This error tends to shift galaxies upwards on the apparent diameter axis. We derived formulae for the bias similar to the classical Malmquist bias. This selection bias in the apparent diameters leads to an overestimation of the $\langle \log H_0 \rangle$. Similar formulae and results are valid for the magnitudes.

In Sect. 5 we asked whether it is possible to devise a mean for deriving the inverse Tully-Fisher parameters if the $\log V_{\text{max}}$ -values are distributed symmetrically, but not normally, around a given X , where X denotes either M or $\log D$. We constructed a normalized “inverse Spaenhauer diagram”. The most important virtue of this diagram is that one can relax the requirement of normally distributed deviations from the mean. The only requirement for the normalization to be successful is that the data-points are symmetric and complete around the common mean. It was also shown that the correct normalization slope indeed corrects for the bias in the distances derived caused by the erroneous slope. We also demonstrated the use of the normalized inverse Spaenhauer diagram. If a selection cut-off at some p exists, it seen in the diagram as a decline of the upper envelope of the normalized p_n -distribution as a function of distance.

In Sect. 6. we asked, what happens if the distribution is neither normal or symmetric. Using a simple mass-model we derived an “expnormal” distribution of $\log V_{\text{max}}$'s. If the Tully-Fisher parameters are solved using least squares from this distribution, one underestimates the zero-point because of the tail of small $\log V_{\text{max}}$ -values. As a result one overestimates the value of H_0 . Finally, if the resulting $\log H_0$ -distribution is asymmetric, $\langle \log H_0 \rangle$ does not anymore reflect the correct $\langle H_0 \rangle$.

Acknowledgements. The question of an asymmetric $\log V_{\text{max}}$ distribution was raised during the visit of T.E. to the Observatory of Meudon. He would like to thank L. Gouguenheim, L. Bottinelli and G. Theureau for their hospitality during the visit. The authors would also like to thank L. Gouguenheim for her useful comments.

References

- Bottinelli, L., Gouguenheim, L., Patrel, G., Teerikorpi, P., 1986, A&A, 156, 157
 Dyson, F., 1926, MNRAS, 86, 686
 Gould, A., 1993, ApJ, 412, L55
 Ekholm, T., 1996, A&A, 308, 7 (Paper I)
 Patrel, P., Bottinelli, L., Di Nella, H., et al., 1994, A&A, 289, 711
 Perryman, M. A. C., Lindegren, L., Kovalevsky, J., et al., 1995, A&A, 304, 69
 Sandage, A., 1994a, ApJ, 430, 1
 Sandage, A., 1994b, ApJ, 430, 13
 Teerikorpi, P., 1984, A&A, 141, 407
 Teerikorpi, P., 1990, A&A, 234, 1
 Teerikorpi, P., 1993, A&A, 280, 443
 Teerikorpi, P., 1995, Astrophys. Lett. Commun., 31, 263
 Theureau, G., Hanski, M., Teerikorpi, P., et al., 1997a, A&A, in press
 Theureau, G., Hanski, M., Ekholm, T., et al., 1997b, A&A, in press